

# Glass matrix/pyrochlore phase composites for nuclear wastes encapsulation

A. A. DIGEOS

*Department of Materials, Imperial College, London SW7 2BP, UK*

J. A. VALDEZ, K. E. SICKAFUS

*MS-G755, Los Alamos National Laboratory, Los Alamos, NM 87545, USA*

S. ATIQ, R. W. GRIMES, A. R. BOCCACCINI\*

*Department of Materials, Imperial College, London SW7 2BP, UK*

*E-mail: a.boccaccini@ic.ac.uk*

Novel composite materials have been developed as alternative forms to immobilise nuclear solid waste. These composites are made of a lead-containing glass matrix, into which particles of lanthanum zirconate pyrochlore are embedded in 10 and 30 vol% concentrations. The fabrication involves powder mixing, pressing and pressureless sintering. The processing conditions were investigated with the aim of achieving the highest possible density. The best composites obtained showed a good distribution of the lanthanum zirconate particles in the glass matrix, strong bonding of the particles to the matrix and relatively low porosity (<10%). The best sintering temperature was 600°C for the 10 vol% composite and 650°C for 30 vol%. Sintering was carried out for an hour and a heating rate of 10°C · min<sup>-1</sup> was shown to be superior to a heating rate of 2°C · min<sup>-1</sup>. At the relatively low sintering temperatures used, the pyrochlore crystalline structure of lanthanum zirconate, relevant for containment of radioactive nuclei, was stable.

© 2003 Kluwer Academic Publishers

## 1. Introduction

An issue of concern in the development of vitreous waste forms for nuclear waste encapsulation is the partial devitrification of the glass over time [1]. In such circumstances it is probable that certain of the waste elements partition into the crystalline component of what is now a glass ceramic [2]. Amongst other problems [1], with further aging, the crystalline phase may undergo amorphization which leads to swelling and will induce micro-cracking [3].

Recently there has been renewed interest in using materials with fluorite and fluorite related structures such as pyrochlore as possible host phases for fission products and actinides, in particular Pu [4–7]. Certain of these materials have been shown to be remarkably stable against heavy ion induced amorphization. For example, it was not possible to amorphize Er<sub>2</sub>Zr<sub>2</sub>O<sub>7</sub> even after irradiation by 350 keV Xe<sup>++</sup> ions to a fluence of 5 × 10<sup>16</sup> ions/cm<sup>2</sup>, equivalent to over 150 displacements per ion [8].

Interestingly (Gd,Cm)<sub>2</sub>Ti<sub>2</sub>O<sub>7</sub> pyrochlore has been observed as a devitrification product in a glass waste form [3]. However, the parent phase Gd<sub>2</sub>Ti<sub>2</sub>O<sub>7</sub> does undergo radiation induced amorphization both in a glass-ceramic [9] and as a pure phase [10]. Pyrochlore phases also form in a Synroc waste form as one of a multitude

of phases [11]. Furthermore, it has been proposed that Synroc could be combined with a glassy phase to form a composite waste form [11]. More recently, reaction sintered glass has been developed as a durable matrix for spinel-forming nuclear waste compositions [12]. Finally, a ceramic-glass composite waste form has been developed at Argonne National Laboratory although in this case the crystalline phase is an aluminosilicate zeolite which is then combined with 25% glass frit and hot isostatically pressed [13].

Given the above developments and experience, it seems sensible to consider forming a simple ceramic-glass composite which incorporates a more radiation resistant zirconate pyrochlore. Thus, here we will demonstrate the fabrication of La<sub>2</sub>Zr<sub>2</sub>O<sub>7</sub> pyrochlore-glass composites. In fact, La<sub>2</sub>Zr<sub>2</sub>O<sub>7</sub> has been shown experimentally not to be the most radiation resistant pyrochlore [14], which agrees with earlier predictions [15, 16]. However, even more resistant materials such as Gd<sub>2</sub>Zr<sub>2</sub>O<sub>7</sub>, in other ways, exhibit very similar physical properties. In particular, the thermal expansivities are almost identical and extremely well matched to the selected glass matrix (see Table I and references [17–19]). One problem with using crystalline ceramics is that only selected fission products and actinides are readily soluble in a specific lattice. In particular,

\* Author to whom all correspondence should be addressed.

TABLE 1 Comparison of some physical properties of TV cone glass [17] and  $\text{La}_2\text{Zr}_2\text{O}_7$  [18, 19]

	$\text{La}_2\text{Zr}_2\text{O}_7$	Television set cone glass
Density ( $\text{g}/\text{cm}^3$ )	6.05	2.89
Melting/softening point ( $^\circ\text{C}$ )	2300	580
Thermal expansion coefficient ( $10^{-6} \text{K}^{-1}$ )	9.1 (30–1000 $^\circ\text{C}$ )	9.1–9.3

pyrochlores have an affinity for rare earth ions and have been proposed as useful materials for the disposition of actinides such as Pu [20]. As such, the type of waste form we propose may well find particular use with certain weapons based legacy waste. On the other hand, if a suitably durable glass could be identified, the composite may accommodate other shorter lived fission products (e.g., Cs and I) in that glass.

The use of glass for the matrix has the important advantage of allowing relatively low processing temperatures ( $<800^\circ\text{C}$ ), which are much lower than the sintering temperature required for densification of pyrochlore crystalline ceramics. These glass powder compacts are densified by exploiting a low-temperature viscous flow sintering mechanism [21]. This could be an important benefit if elements such as Am are to be contained which exhibit low volatilisation temperatures.

The glass chosen for this investigation is a glass cullet recovered from television (TV) set cones. Such glass is itself a surplus material with associated environmental issues [22]. In particular, the glass contains a significant level of lead (about 10 wt% PbO) [16]. As such, it will interact with the radiation flux generated by any nuclear waste. This may be beneficial or detrimental depending on the fission product and/or actinide inventory and post irradiation history (i.e., it may provide some  $\alpha$  or  $\beta$  shielding but also facilitate the formation of activated products or modification of absorption cross-sections of radiations). However, given the conventional processing, based on powder technology and sintering, fabrication does not require expensive or complex equipment.

It is noted that the amount of electronic waste glasses available, in particular Pb-containing glasses from television set cones [22], would guarantee sufficient material available for the preparation of the matrix in the present waste encapsulation process and at the same time provide a useful application for these problematic glass residues.

## 2. Experimental procedure

### 2.1. Materials

The lanthanum zirconate powder was prepared from individual powders of  $\text{La}_2\text{O}_3$  (Alpha Aesar 99.99% purity) and  $\text{ZrO}_2$  (Alpha Aesar 99.978% purity) calcined at  $1000^\circ\text{C}$  for 24 hours. Powders were measured in stoichiometric proportions and placed in a plastic vial. They were then mixed for 6 hours in a spex mill. Following this the mixed powders were put in a  $\text{ZrO}_2$  vial with one  $\text{ZrO}_2$  ball and ball milled for 2 hours. Powders were then pressed in a stainless steel die of

13 mm diameter at a constant pressure of 700 MPa for 15 minutes. The pressed pellets were subsequently placed in a furnace for 24 hours at  $1200^\circ\text{C}$ . These pellets were removed from the furnace then re-milled and re-pressed under the same conditions stated above. The pellets were placed in a furnace for a second heat treatment for 48 hours at  $1650^\circ\text{C}$ . Lanthanum zirconate powder was obtained by crushing and powdering the sintered pellets by using a mortar and a pestle. The morphology of the powder used to fabricate the composites was analysed by scanning electron microscopy (SEM) using a JEOL JSM-T 220 microscope, working at 25 kV, using 20 mm as the working distance. The lanthanum zirconate powder was also analysed by X-Ray Diffraction (XRD), using a Philips PW 1719 ( $\text{Cu K}_\alpha$  radiation, current: 40 mA, tube voltage: 40 kV). A second XRD analysis was made after calcination of the powders in both air and in argon at  $800^\circ\text{C}$ , in order to detect any phase transformation that may have occurred.

The lead-containing glass was obtained from discarded TV sets. In particular, glass cullet from a TV set cone was selected. The glass powder of average particle size  $2 \mu\text{m}$  was obtained using a ball mill. This glass was chosen primarily because its thermal expansion coefficient matches that of lanthanum zirconate and given its relatively high Pb content (PbO content: 9.8 wt%), it exhibits high sinterability at relative low temperatures ( $<700^\circ\text{C}$ ) [17]. Moreover, due to current difficulties to recycle these glasses and the environmental concern due to their heavy metal content [22], there is strong interest to develop alternative technologies for their reuse. Table 1 shows a summary of some relevant properties of the two materials used for the present composites.

### 2.2. Preparation of composite samples

Two powder mixtures were prepared by adding 10 and 30 vol% of lanthanum zirconate respectively to the glass powder. These mixtures were dry-mixed for half an hour in a tubular mixer. Cylindrical samples were then uniaxially dry-pressed using a pressure of 100 MPa in a stainless steel die of 8 mm diameter. Samples of about 3–4 mm height were obtained. The pressing time was optimised to avoid the appearance of delamination in the samples. A release agent (Buehler, No 20-8185-016) was used on the wall of the steel die to facilitate the extraction of the samples.

The sintering process of the composites was optimised to determine the temperature, time and heating rate required to obtain high-density samples. Previous work on the sintering of the glass powder [17], was used as the basis on which initial parameters and parameter ranges were selected. At least 20 different samples of each composition were submitted to sintering experiments. They were heated at different temperatures in the range  $550$ – $680^\circ\text{C}$  for an hour, using heating rates of  $10^\circ\text{C} \cdot \text{min}^{-1}$  and  $2^\circ\text{C} \cdot \text{min}^{-1}$ .

### 2.3. Characterisation of the composites

The density of each sample was determined geometrically and by the Archimedes' method and subsequently compared to the theoretical density in order

to determine the level of porosity. The samples were weighted with a precision of  $10^{-4}$  g. The theoretical density of the composites was obtained using the “mixtures rule.”

Tiny fragments of sintered samples were crushed into powder for X-Ray diffraction analysis. Both fractured samples and polished samples were analysed by SEM. EDX analyses were carried out on polished samples. For polishing, selected samples were mounted in a resin matrix, ground with SiC paper and then polished for half an hour with  $1\ \mu\text{m}$  diamond paste.

### 3. Results and discussion

#### 3.1. Characterisation of the lanthanum zirconate powder

XRD analyses showed that the as received ceramic powder consisted of lanthanum zirconate crystals, with a small amount of lanthanum hydroxide, as shown in Fig. 1. The XRD analyses of samples calcined in air and in argon at  $800^\circ\text{C}$  for 2 h are compared with the as-received sample spectrum in Fig. 2. The three superimposed spectra coincide in all fundamental peaks. Thus the lanthanum zirconate powder is thermally

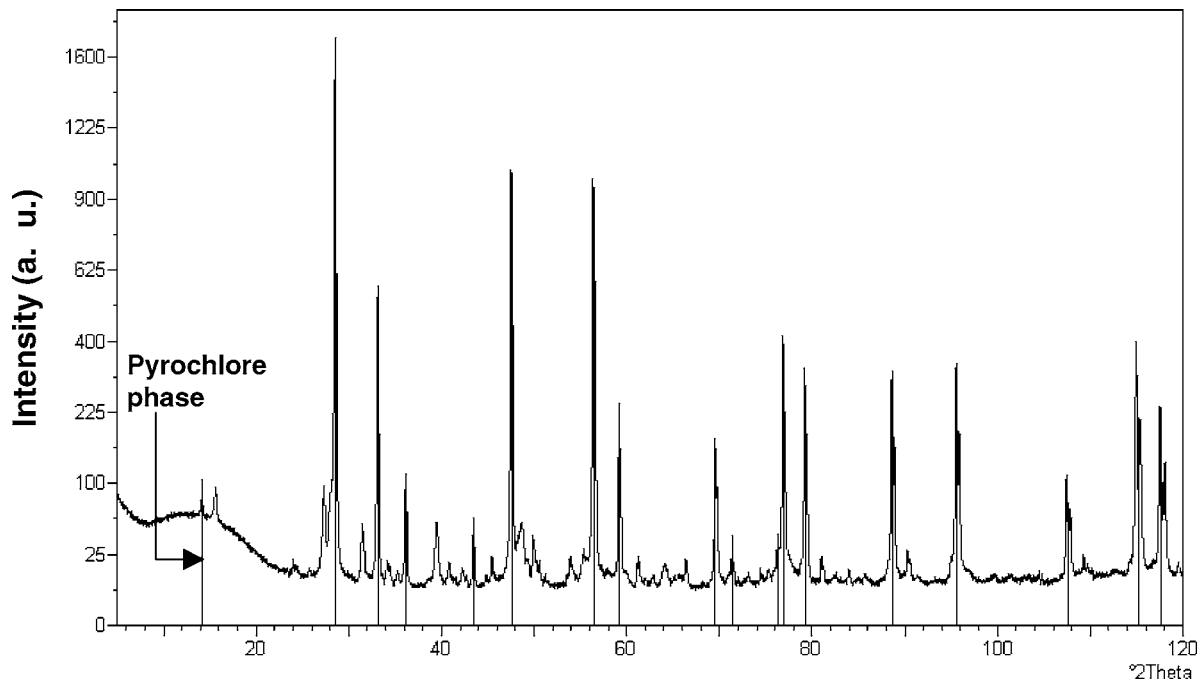


Figure 1 XRD spectrum of the lanthanum zirconate material used, confirming stoichiometric pyrochlore crystalline structure.

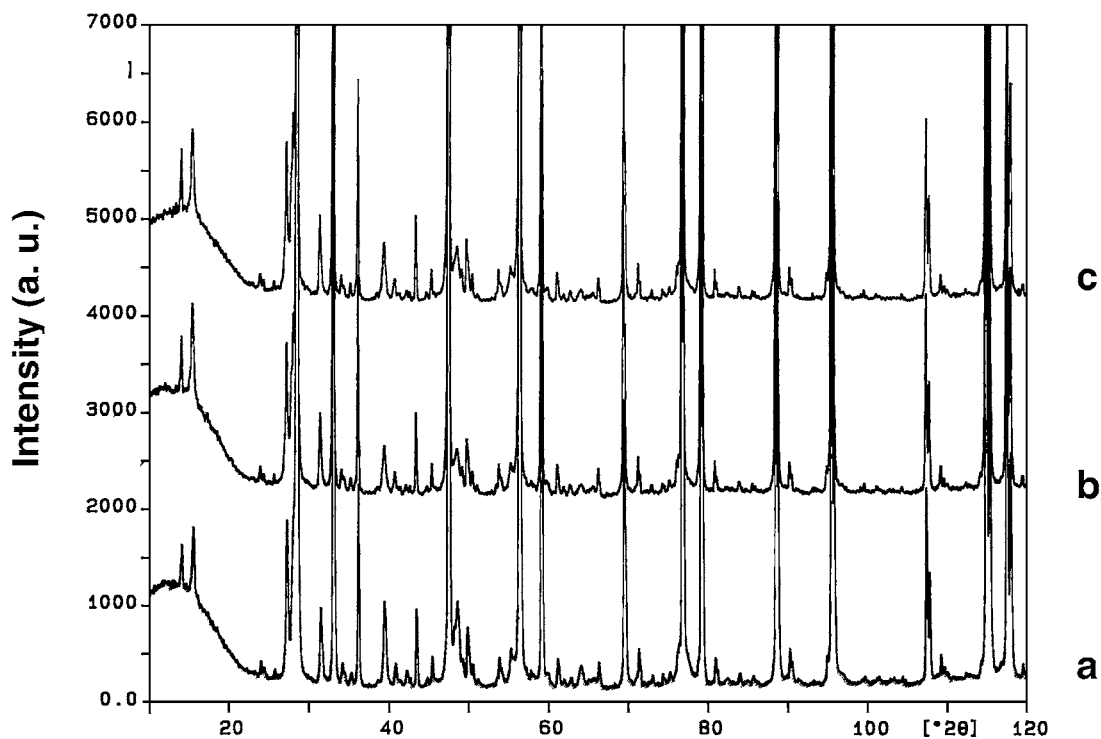
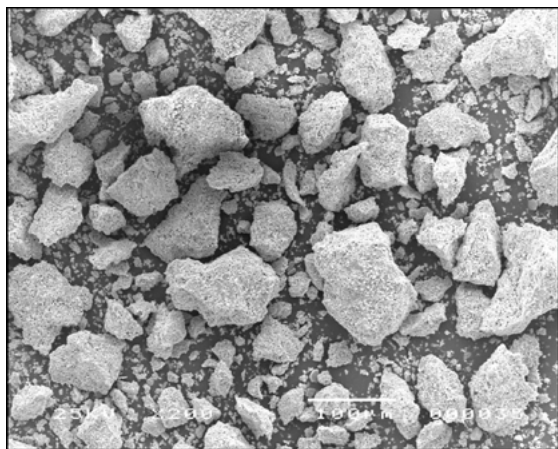
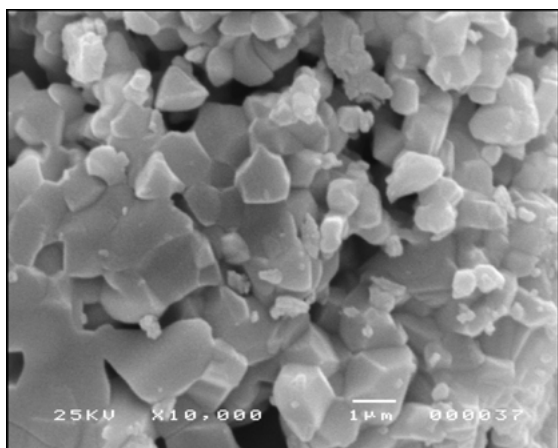


Figure 2 XRD spectra of the lanthanum zirconate powder: (a) original powder, (b) after calcination in air at  $800^\circ\text{C}$  and (c) after calcination in argon at  $800^\circ\text{C}$ .



(a)



(b)

Figure 3 SEM images of the original lanthanum zirconate powder at (a) low and (b) high magnification, showing large agglomerates and their microstructure.

stable until at least 800°C, and will not transform to another structure over the temperature range of interest for this study (i.e., <700°C).

Fig. 3 shows SEM images of the lanthanum zirconate powder. As seen in Fig. 3a, a large number of individual primary particles of lanthanum zirconate have coalesced during the high-temperature fabrication of the powder, leading to the formation of large agglomerates. Fig. 3b shows that the agglomerates are composed of sintered primary particles of sizes in the range 1–10 μm and that they contain considerable residual intergranular porosity.

### 3.2. Characterisation of composites

The sintering temperatures that led to the highest density composites were different for the two compositions. This is due to their different lanthanum zirconate content. Higher particle contents have a stronger effect on sintering densification, as it is well-known from the literature on sintering of glasses containing rigid inclusions [23]. The samples with 30 vol% pyrochlore inclusions required therefore a higher sintering temperature. The density and sintering conditions for both samples are shown in Table II. For both compositions investigated, densities >91% of theoretical were achieved by the simple powder technique employed

TABLE II Optimised sintering conditions and density values obtained (The sintering time was 1 h in all cases)

	Density (g/cm <sup>3</sup> )	Relative density (%)
10 vol% composite sintered at 600°C	2.95	92.0
Heating rate: 10°C/min		
10 vol% composite sintered at 600°C	2.38	74.1
Heating rate: 2°C/min		
30 vol% composite sintered at 650°C	3.51	91.4
Heating rate: 10°C/min		
30 vol% composite sintered at 650°C	2.66	69.2
Heating rate: 2°C/min		

here using a heating rate of 10°C/min, which should therefore warrant adequate structural integrity of the composites.

The XRD pattern of a typical composite sample containing 10 vol% lanthanum zirconate and sintered at 600°C is shown in Fig. 4a. Also shown in this figure are the positions of the main pyrochlore peaks. Fig. 4b shows the XRD spectrum of the original lanthanum zirconate powder superposed onto the pattern of the composite sample. It is clear from these figures that no new crystalline phases have formed during sintering. Moreover, the sintering procedure at 600°C has not altered the crystalline pyrochlore structure of the initial lanthanum zirconate particles.

The SEM analyses of the sintered composites have led to several interesting observations. As shown in Fig. 5a, for the composite containing 10 vol% particles, there is a homogeneous distribution of the lanthanum zirconate particles in the glass matrix. Moreover, in agreement with the density measurements, only limited porosity is observed in this sample. By analysing fracture surfaces of sintered samples, information on crack propagation can be obtained, especially regarding the fracture propagation at the interface between matrix and particles. Fig. 5a and b show the fracture surface of the 10 vol% composite at low and intermediate magnifications, respectively. It is clear that fracture has proceeded through the lanthanum zirconate particles. There is consequently neither crack-deflection at the interface nor debonding or pull-out of the particles, with the advancing crack propagating directly through the particles. Qualitatively this indicates a strong bonding at the interface between the matrix and particles, which is relevant regarding both the mechanical and chemical stability of the samples. Fig. 5a and b also show that this composite contains two types of porosity. There are a few isolated pores in the matrix (Fig. 5a), left possibly by gas entrapment during sintering densification, but there is also residual porosity between the primary lanthanum zirconate particles inside the agglomerates. This becomes clear in Fig. 5c, which shows that the porosity is similar to that inside the starting agglomerates (Fig. 3b). This also indicates that no significant densification of the lanthanum zirconate particles has occurred during composite sintering, as expected given the relatively low temperature used (600°C).

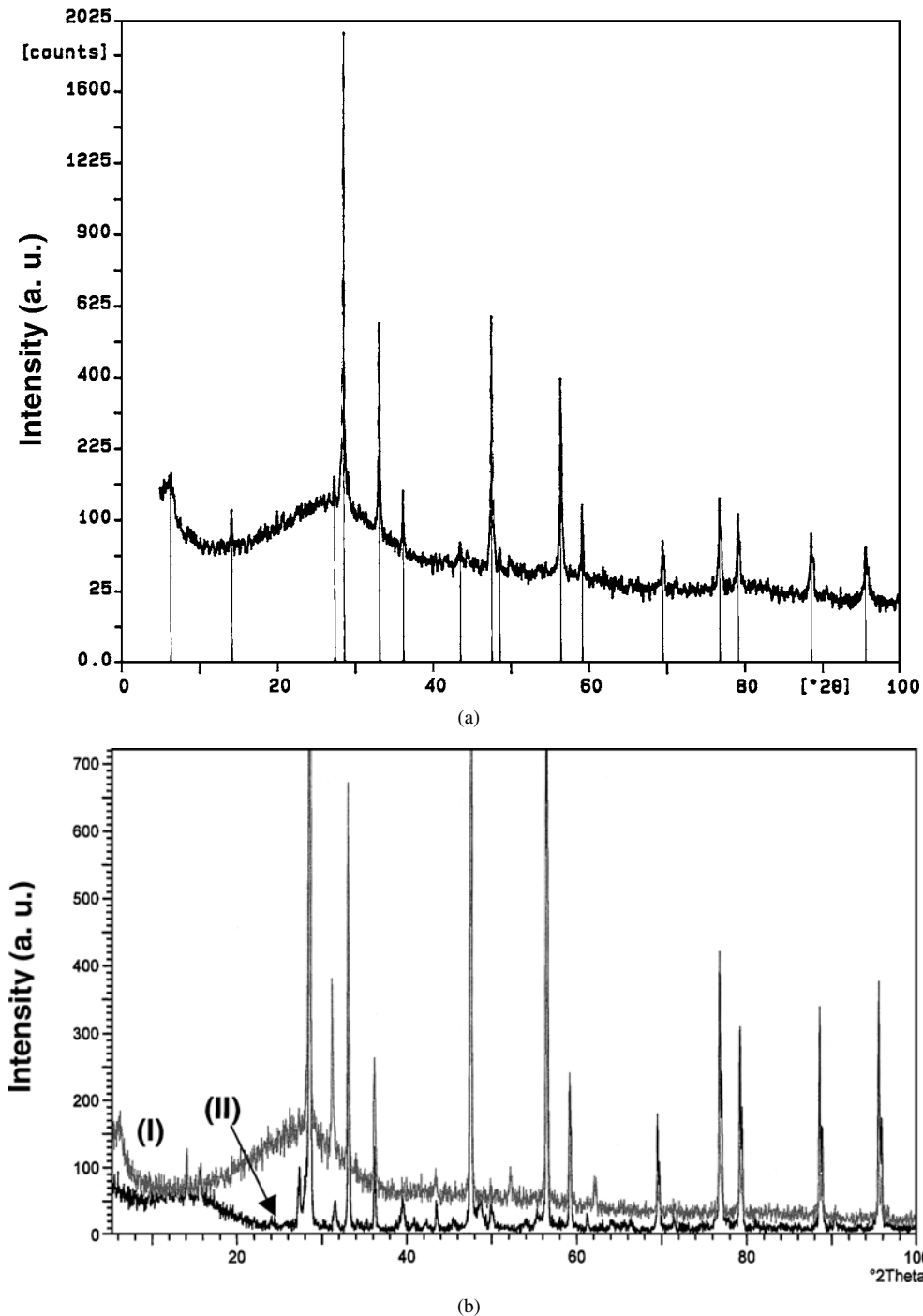
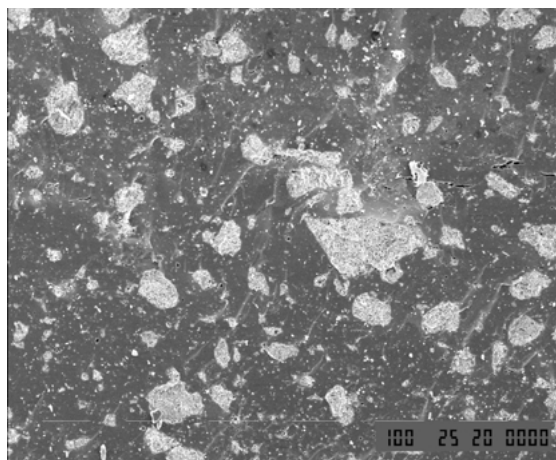


Figure 4 (a) XRD pattern of a composite sample containing 10 vol% lanthanum zirconate obtained via sintering at 600°C with a heating rate of 10°C · min<sup>-1</sup>. The pattern of lanthanum zirconate of pyrochlore structure is also shown for comparison. (b) XRD patterns of (I) the composite sample of (a) and (II) the pattern of the original lanthanum zirconate powder of pyrochlore structure.

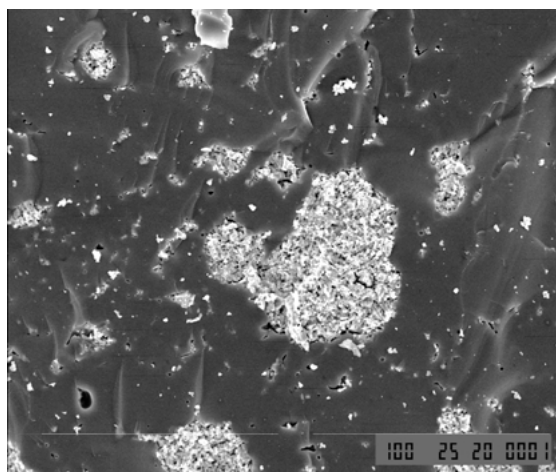
Polished samples containing 30 vol% lanthanum zirconate particles, which have been sintered at two different heating rates are shown in Fig. 6. The distribution of lanthanum zirconate particles in the glass matrix is homogeneous in both samples. It is clearly seen that heating at a lower rate (see Fig. 6b) led to higher porosity (compare to Fig. 6a). In these samples also the particles are seen to be well bonded to the glass matrix. The interface bonding seems to be qualitatively very strong, as there has been no debonding of the particles during polishing. EDX analyses of these samples revealed that the composition of the glass remained stable, and that lanthanum zirconate particles have also maintained the same composition during the sintering process. Re-

sults for a sample sintered at 650°C at a heating rate of 10°C /min are shown in Fig. 7.

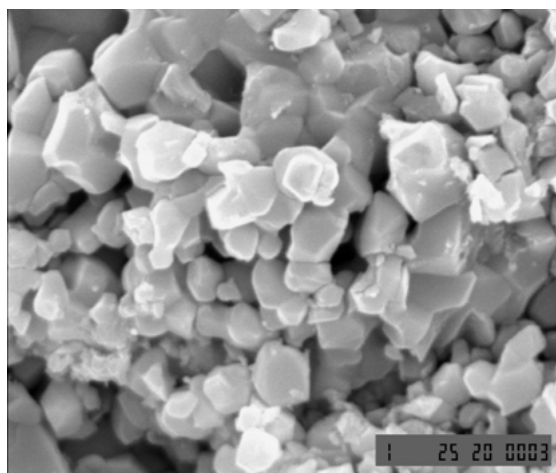
Finally, it should be mentioned that no major development of sintering defects, such as microcracks or crack-like voids were observed in the samples. This suggests that the composite materials will have good mechanical strength and structural integrity, although the mechanical properties were not determined in this study. Indeed the use of a glass matrix with a thermal expansion coefficient close to that of the lanthanum zirconate particles (see Table I) should avoid the development of thermal cracks during cooling from the sintering temperature. The similar thermal conductivities of the matrix glass and pyrochlore particles will



(a)



(b)

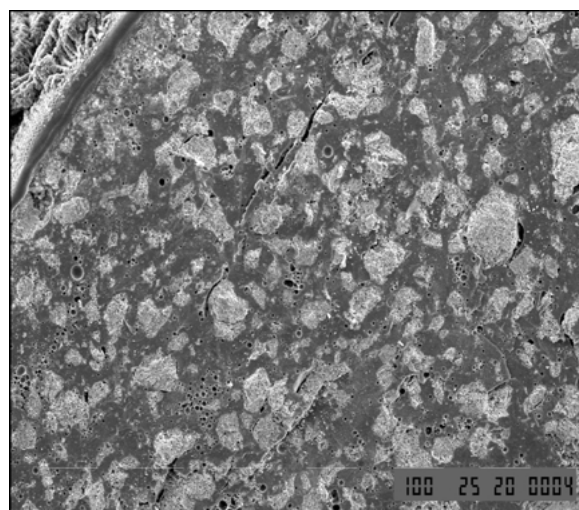


(c)

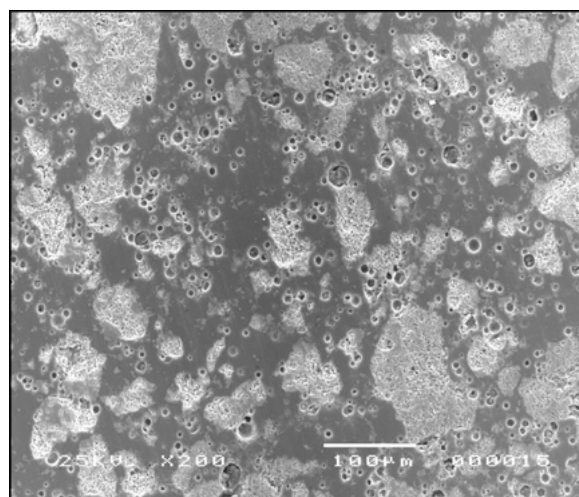
Figure 5 SEM micrographs of the fracture surface of a sintered composite with 10 Vol% lanthanum zirconate obtained by sintering at 600°C at a heating rate of 10°C/min, at different magnifications, showing: (a) homogeneous distribution of the lanthanum zirconate particles in the glass matrix and low matrix porosity, (b) propagation of fracture in the matrix and through the lanthanum zirconate particles, and (c) porosity inside an agglomerate of lanthanum zirconate particles.

also avoid discontinuous changes in thermal gradient at the glass/particle interface.

The absence of residual thermal stresses in the composite may also explain the rather planar fracture surfaces (Fig. 5a and b), without noticeable crack deflection at the particle/matrix interfaces, which is a



(a)



(b)

Figure 6 SEM micrographs of polished samples of composites containing 30 vol% lanthanum zirconate sintered at 650°C at heating rates of (a) 10°C/min and (b) 2°C/min.

typical effect observed in particle reinforced glasses with thermal expansion mismatch [24]. Future work will focus on the characterisation of temperature-dependant hardness, toughness and fracture strength of the fabricated composites. It also remains to be determined whether or not the lanthanum zirconate particles may impart toughening and impact resistance to these materials by, for example, the direct particle cutting toughening mechanism [25]. The significance of primary pyrochlore particle agglomeration and residual porosity will also be considered further. After the comprehensive assessment of the mechanical behaviour of these novel composites, tests are planned to characterise their chemical durability and leaching behaviour, in particular their dependence on pyrochlore phase content.

The chemical durability of lead containing silicate glasses for applications in nuclear waste encapsulation has been much less investigated in comparison to borosilicate and phosphate glasses [26]. There are however indications that lead containing glasses have a lower chemical durability than borosilicate glasses [27]. Indeed at low PbO concentrations, lead

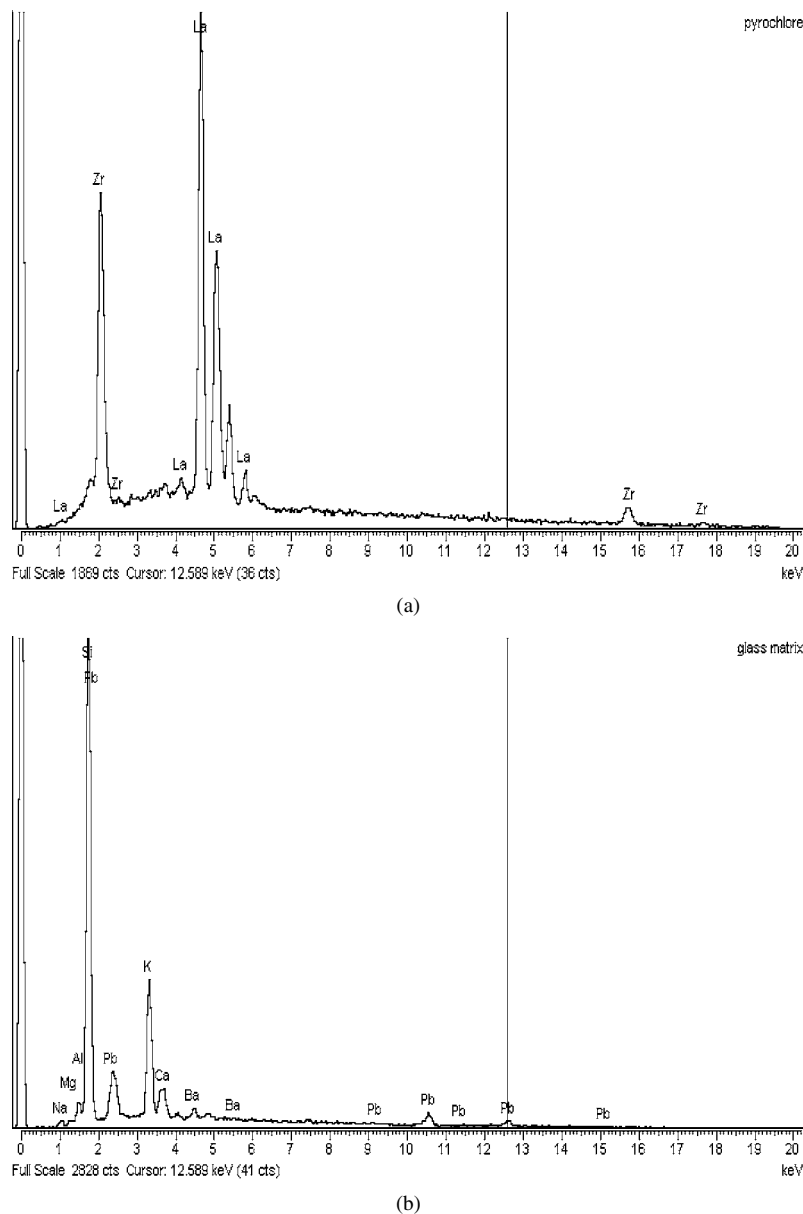


Figure 7 EDAX results on a polished sample containing 30 vol% lanthanum zirconate, sintered at 650°C with a heating rate of 10°C/min. Results for: (a) agglomerate of lanthanum zirconate particles and (b) glass matrix.

is a network modifier and decreases the number of bonds between  $[\text{SiO}_4]^{4-}$  tetrahedra [28]. Despite these findings, the addition of a lead borosilicate glass to alfa-quartz has been attempted in previous waste encapsulation concepts [29] in order to enhance consolidation of the silicate glass mixture during hot pressing. Addition of PbO has been also used in multibarrier systems for the permanent disposal of high-level radioactive waste [30]. In the present waste encapsulation process the glass matrix acts as a second barrier and it is not the host phase for long lived fission products or radionuclides. It may be assumed therefore that a (limited) reduction of chemical durability of the glass in comparison with, for example, borosilicate glasses may be accepted, specially considering the advantages of the lead-containing matrix, which are, as mentioned above, the possibility of low-temperature processing (<700°C), the possibility of radiation shielding as well as the provision of an application possibility for the Pb-containing electronic waste glasses.

#### 4. Conclusions

Novel composites consisting of a lead-containing glass matrix and lanthanum zirconate pyrochlore particles were fabricated and characterised. A glass with thermal expansion coefficient matching that of lanthanum zirconate was chosen. The composites are proposed as alternative waste forms for selected radioactive residues, exploiting the actinide solubility in the pyrochlore phase [6,31 ex 24] and the encapsulating ability of the glass matrix. Powder processing and pressureless sintering at relatively low temperatures (<700°C) were used to fabricate the composites. A uniform distribution of the lanthanum zirconate particles in the glass matrix was achieved. The composites are homogeneous in their microstructure and structurally resistant. Qualitatively, it was found that the lanthanum zirconate particles are well bonded to the glass matrix and that there is no cracking at the interface between glass and lanthanum zirconate particles. The compositions of the lanthanum zirconate particles did not change during the fabrication

process. As the porosity in the final composites is less than 10%, it may be anticipated that this porosity will not significantly affect mechanical strength. The present composites may provide new alternatives for the safe storage of nuclear wastes via a low temperature fabrication route. The chemical durability of the glass matrix/pyrochlore composites containing different volume fractions of pyrochlore phase should be investigated as part of the next development stage of the present materials.

### Acknowledgements

The experimental assistance of Mr. N. Royall and Mr. R. Sweeney (Department of Materials, Imperial College) at different stages of this project is gratefully appreciated.

### References

1. A. K. DE, B. LUCKSCHEITER, W. LUTZE, G. MALOW and E. SCHIEWER, *Ceramic Bull.* **55** (1976) 500.
2. W. J. WEBER, R. P. TURCOTTE and F. P. ROBERTS, *Rad Waste Man.* **2** (1982) 295.
3. W. J. WEBER, R. P. TURCOTTE, L. R. BUNNELL, F. P. ROBERTS and J. H. WESTSIK, JR., in "Radiation Effects in Vitreous and Devitrified Simulated Waste Glass", edited by T. D. Chikalla and J. E. Mendel, CONF-790420 (National Technical Information Service, Springfield, VA, 1979) p. 294.
4. S. X. WANG, B. D. BEGG, L. M. WANG, R. C. EWING, W. J. WEBER and K. V. G. KUTTY, *J. Mater. Res.* **14** (1999) 4470.
5. B. BURAKOV, E. ANDERSON, M. YAGOVKINA, M. ZAMORYANSKAYA and E. NIKOLAEVA, "Behavior of <sup>238</sup>Pu-Doped Ceramics Based on Cubic Zirconia and Pyrochlore Under Radiation Damage," International Conf. ACTINIDES-2001, Hayama, Japan.
6. S. YAMAZAKI, T. YAMASHITA, T. MATSUI and T. NAGASAKI, *J. Nucl. Mater.* **294** (2001) 183.
7. W. L. GONG, W. LUTZE and R. C. EWING, *ibid.* **277** (2000) 239.
8. K. E. SICKAFUS, L. MINERVINI, R. W. GRIMES, J. A. VALDEZ, M. ISHIMARU, F. LI, K. J. MCCLELLAN and T. HARTMANN, *Science* **289** (2000) 748.
9. S. X. WANG, L. M. WANG, R. C. EWING, G. S. WAS and G. R. LUMPKIN, *Nucl. Instrum. Methods Phys. Res. B* **148** (1999) 704.
10. W. J. WEBER, J. W. WALD and H. MATZKE, *Mater. Lett.* **3** (1985) 173.
11. W. J. WEBER, R. C. EWING, C. R. A. CATLOW, T. DIAZ DE LA RUBIA, L. W. HOBBS, C. KINOSHITA, HJ. MATZKE, A. T. MOTTA, M. NASTASI, E. K. H. SALJE, E. R. VANCE and S. J. ZINKLE, *J. Mater. Res.* **13** (1998) 1434.
12. W. L. GONG, W. LUTZE and R. C. EWING, *J. Nucl. Mater.* **278** (2000) 73.
13. D. W. ESH, K. M. GOFF, K. T. HIRSCHE, T. J. BATTISITI, M. F. SIMPSON, S. G. JOHNSON and K. J. BATEMAN, *Mater. Res. Soc. Symp. Proc.* **556** (1999) 107.
14. J. LIAN, X. T. ZU, K. V. G. KUTTY, J. CHEN, L. M. WANG and R. C. EWING, *Phys. Rev. B* **66** 0541XX-1 (2002) in press.
15. L. MINERVINI, R. W. GRIMES and K. E. SICKAFUS, *J. Amer. Ceram. Soc.* **83** (2000) 1873.
16. M. PIRZADA, R. W. GRIMES, L. MINERVINI, J. F. MAGUIRE and K. E. SICKAFUS, *Solid State Ionics* **140** (2001) 201.
17. A. R. BOCCACCINI, M. BUECKER, P. A. TRUSTY, M. ROMERO and I. M. RINCON, *Glass Technol.* **38**(4) (1997) 128.
18. J. NAIR, P. NAIR, G. B. M. DOESBURG J. G. VAN OMMEN, J. R. H. ROSS, A. J. BURGGRAAF and F. MIZUKAMI, *J. Amer. Ceram. Soc.* **82**(8) (1999) 2066.
19. R. VASSEN, *ibid.* **83**(8), (2000) 2023.
20. W. J. WEBER and R. C. EWING, *Science* **289** (2000) 2052.
21. G. W. SCHERER, *J. Amer. Ceram. Soc.* **60** (1977) 239.
22. J. M. HERMANS, J. G. J. PEELEN and R. BEI, *Ceram. Bull.* **80**(3) (2001) 51.
23. G. W. SCHERER, *ibid.* **70** (1991) 1059.
24. A. R. BOCCACCINI and P. A. TRUSTY, *J. Mater. Sci. Lett.* **15** (1996) 60.
25. A. R. BOCCACCINI, *Ceramica Acta* **8**(1) (1996) 5.
26. I. W. DONALD, B. L. METCALFE and R. N. J. TAYLOR, *J. Mater. Sci.* **32** (1997) 5851.
27. W. LUTZE and R. C. EWING (eds.), "Radioactive Waste Forms for the Future" (North Holland, Amsterdam, 1988).
28. E. M. RABINOVICH, *J. Mater. Sci.* **11** (1976) 925.
29. G. J. MCCARTHY and M. T. DAVIDSON, *Ceram. Bull.* **55** (1976) 190.
30. S. S. KIM, J. G. LEE, I. K. CHOI, G. H. LEE and K. S. CHUN, *Radiochim. Acta* **79** (1997) 199.
31. I. HAYAKAWA and H. KAMIZONO, *Mater. Res. Soc. Symp.* **257** (1992) 257.

Received 16 October 2002  
and accepted 16 January 2003